Available online at www.sciencedirect.com

ScienceDirect

Solid Earth Sciences 1 (2016) 64–73

www.elsevier.com/locate/SESCI

Oceanic anoxic events, subduction style and molybdenum mineralization

Wei-dong Sun [a,b,*], Cong-ying Li [a], Xi-luo Hao [a], Ming-xing Ling [c], Trevor Ireland [d], Xing Ding [c], Wei-ming Fan [b]

[a] *Key Laboratory of Mineralogy and Metallogeny, Guangzhou Institute of Geochemistry, Chinese Academy of Sciences, 511 Kehua Street, Wushan, Guangzhou 510640, China*

[b] *CAS Center for Excellence in Tibetan Plateau Earth Sciences, The Chinese Academy of Sciences, Beijing 100101, China*

[c] *State Key Laboratory of Isotope Geochemistry, Guangzhou Institute of Geochemistry, Chinese Academy of Sciences, 511 Kehua Street, Wushan, Guangzhou 510640, China*

[d] *Research School of Earth Sciences, The Australian National University, Bldg 61 Mills Road Acton ACT, Canberra, ACT 0200, Australia*

Available online 14 January 2016

Abstract

Nearly half of the world's Mo resources are hosted in Cenozoic porphyries along the east Pacific margin. In contrast, there are essentially no large Mo porphyry deposits along the west Pacific. We propose that this uneven distribution is mainly due to Oceanic Anoxic Events (OAEs) and the different subduction regimes in the eastern and western Pacific margins. Molybdenum is rare in the Earth, with an abundance of 50 ppb in the primitive mantle, and 0.8 ppm in the continental crust. Pre-enrichment is needed for such a moderately incompatible element to form porphyry Mo deposits. The oxidation–reduction cycle on the Earth's surface is the major process that concentrates Mo. Molybdenum was more intensively oxidized under high erosion rates during alternating high-atmospheric-CO_2 and high-oxygen periods immediately before OAEs, resulting in high Mo concentrations in surface water and subsequently higher Mo concentrations in organic-rich sediments during the OAEs. Large amounts of Mo-enriched sediments formed on the Pacific Ocean floor during at least 9 major OAEs since the Late Jurassic. Given that Mo comes from chemical weathering, far more Mo-enriched sediment was available in the east Pacific because of the erosion of the continental arc. In contrast, due to backarc extension, erosions in the Western Pacific margin was less extensive, resulting in less Mo in OAE sediments on the Pacific Ocean floor. Importantly, the Eastern Pacific plate has been mostly subducted, with only Cenozoic crust left. During plate subduction, large amount of the Mo-rich sediments in the Eastern Pacific have been taken down to the mantle wedge. Subsequently these sediments were metamorphosed and then Mo was transferred to porphyry deposits through partial melting. In contrast, only a small amount of the sediment in the Western Pacific has been subducted, with most of the Jurassic and Cretaceous oceanic crust well preserved.

Molybdenum deposits of the Eastern Pacific margin can be classified into three types: porphyry-Cu-Mo, high-F porphyry and low-F porphyry-Mo deposits. Large and superlarge porphyry-Cu-Mo deposits are usually associated with ridge subductions, and thus formed through partial melting of subducted oceanic crust and metamorphosed Mo-rich sedimentary material due to subduction erosion. The high-F porphyry-Mo deposits (e.g., Climax-type) were likely formed by partial melting of subducted and thus metamorphosed Mo-enriched sediments during slab rollback (usually associated with A-type granite). Low-F porphyry-Mo deposits were formed through direct partial melting of metamorphosed Mo-enriched sediments entrained into the mantle wedge through subduction erosion at slightly shallower depths (usually associated with arc granite). Porphyry-Cu (Au) deposits in the southwest Pacific margin are all associated with subduction of backarc basins younger than the last OAE (55.8 Ma). Therefore, porphyry Cu (Au) deposits in the southwest Pacific margin have no economic levels of Mo. The oxygen fugacity of northwest Pacific is lower than ΔFMQ +2, which inhibits the formation of porphyry deposits.

Keywords: Porphyry Mo deposits; Oceanic anoxic events; Weathering; Pacific; Cretaceous; Jurassic: black shale; Subduction erosion

* Corresponding author. Key Laboratory of Mineralogy and Metallogeny, Guangzhou Institute of Geochemistry, Chinese Academy of Sciences, 511 Kehua Street, Wushan, Guangzhou 510640, China.

E-mail address: weidongsun@gig.ac.cn (W.-d. Sun).

Peer review under responsibility of Guangzhou Institute of Geochemistry.

http://dx.doi.org/10.1016/j.sesci.2015.11.001

1. Introduction

Molybdenum (Mo) is one of the most important elements for modern society because of its variable properties that allow it to make materials ranging from super-hard alloys to solid lubricants. There are three main types of Mo deposits, high-F porphyry Mo, low-F porphyry Mo, and porphyry Cu–Mo deposits. Remarkably, half of the world's Mo resources are hosted in Cenozoic porphyries along the east Pacific margin (Fig. 1). In contrast, there are hardly any large Mo deposits along the west Pacific margin, whereas more than one third of the world's Mo sources are hosted in Cretaceous porphyry Mo deposits in the Triassic Qinling-Dabie orogenic belt (Chen et al., 2000; Li et al., 2012, 2007; Zhang et al., 2014). The formation of Mo deposits along the west coast of the North and South American continents has been attributed to different mechanisms: melting of underplated mafic/ultramafic rocks or intermediate crustal/organic-poor sedimentary rocks (Stein et al., 2001); addition of ore-forming fluids from large Mo enriched magma chambers that crystallized and fractionated in the lower crust or at mid-crustal levels well below the porphyry Mo deposits (Klemm et al., 2008), or subduction-related magmatism (Ludington et al., 2009). However, the details of the mechanism that enriched Mo within a short period of time in such a limited space remain obscure. Here we show that subducted Mo-enriched sediments, which formed during Oceanic Anoxic Events (OAEs), were responsible for the large Mo deposit belt along the eastern Pacific margin. Metamorphism of Mo-rich sediments during subduction is another key factor that controls porphyry Mo deposits.

2. Molybdenum enrichment

Molybdenum is a very rare element with an abundance of only ~50 parts per billion (ppb) in the silicate Earth (McDonough and Sun, 1995), which is only ~0.1% of that of Cu. As a moderately incompatible chalcophile element, Mo is enriched in the continental crust during mantle magmatic processes (McDonough and Sun, 1995; Sun and McDonough, 1989; Sun et al., 2003b), but only by a factor of ~15 compared to the primitive mantle (Rudnick and Gao, 2003) to a level of ~0.8 parts per million (ppm). Nonetheless, Mo forms independent porphyry-Mo deposits with grades up to 0.3% of Mo metal, which is more than 3500 times higher than its abundance in the continental crust. Considering the similarities of Mo and Cu during magmatism and hydrothermal processes, it is surprising that the Mo concentration can be increased by more than 3 orders of magnitude during magmatic and/or hydrothermal processes without concomitant enrichment of Cu.

One of the most important ways that Mo can be concentrated and fractionated from Cu is through the oxidation–reduction cycle during chemical weathering on the surface of the Earth. During weathering, molybdenum is readily oxidized to form water-soluble MoO_4^{2-} in surface environments (Sun et al., 2015b), after the second major elevation of atmospheric oxygen in the Earth's history that occurred

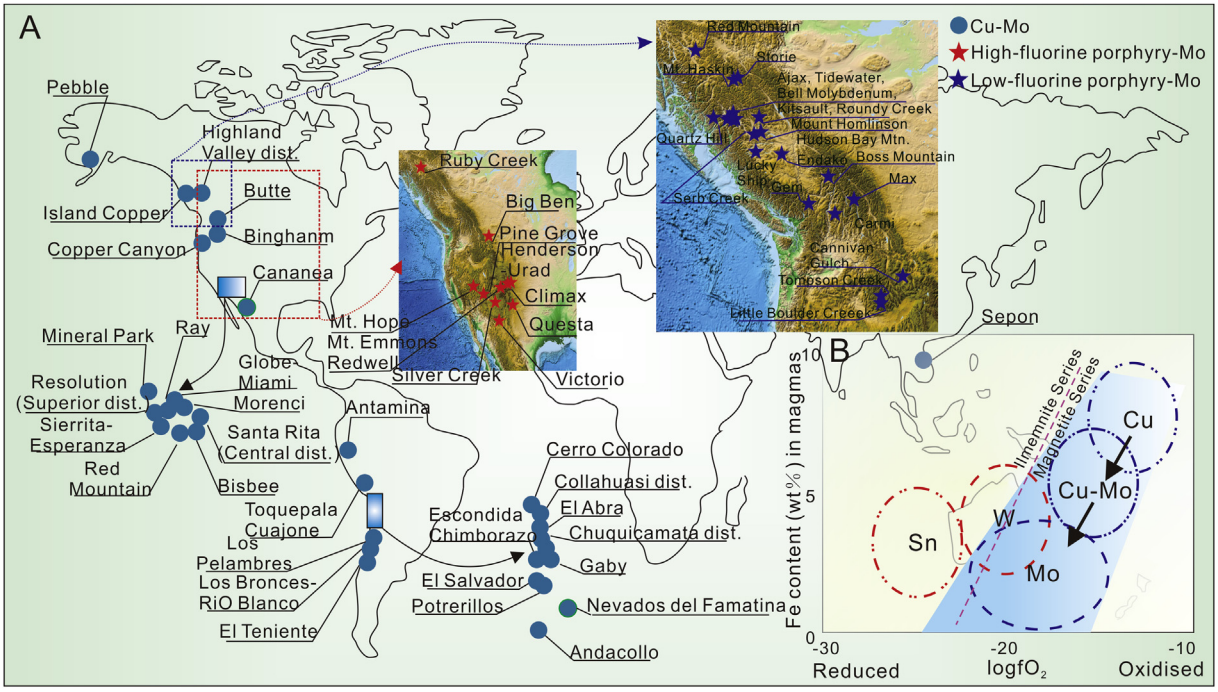

Fig. 1. A. The distribution of porphyry Mo deposits along the Pacific margins. Most of the porphyry-Cu-Mo deposits are closely associated with ridge subductions (Sillitoe, 2010; Sun et al., 2010). High-F porphyry-Mo deposits are found mainly in the Colorado mineral belt (COMB), which was a backarc basin in the Cretaceous and thus collected abundant Mo enriched sediments especially during the oceanic anoxic events (OAEs) (Ludington and Plumlee, 2009). Low-F porphyry-Mo deposits are closely related to porphyry-Cu deposits, but with low Cu contents (Ludington et al., 2009). B. Diagram of Fe versus oxygen fugacity, illustrating that porphyry-Cu-Mo deposits are systematically more oxidizing with higher Fe than porphyry-Mo deposits.

~550 Myr ago (Kump, 2008; Scott et al., 2008; Tribovillard et al., 2006). Water-soluble MoO_4^{2-} is transported to oceans and lakes, and then, through interaction with anoxic sediments it precipitates and is retained to form Mo sulfides/complexes (Fig. 2). As an extreme example, Mo contents could reach weight percent levels in Mo-rich black shales formed immediately after the Snowball Earth in south China (Jiang et al., 2009; Mao et al., 2002; Wille et al., 2008).

In general, reduced water bodies with large catchment areas and high chemical weathering rates are favorable places for the formation of Mo enriched sediments, due to anoxic environments and Mo-rich surface water. Given that chemical weathering is far more intense in tropical regions (Ma et al., 2007), and that developing orogenic belts are usually much more unstable and thus more easily eroded, developing orogens in tropical or sub-tropical regions should be the best suppliers of MoO_4^{2-} to surface waters. In addition, copious amounts of vegetation can act as reducing agents in waters. Such a scenario, however, operates on a local scale, and cannot readily explain the gigantic Cenozoic Mo deposit belt along the western coasts of the American continents.

3. Oceanic anoxic events

Nine major OAEs are recorded in the Jurassic and the Cretaceous, including those of the early Toarcian (~183 Ma), early Aptian (~120 Ma), early Albian (~111 Ma), and Cenomanian–Turonian (~93 Ma) (Alberdi-Genolet and Tocco, 1999; Jenkyns, 2010; McElwain et al., 2005; Scopelliti et al., 2006; Suan et al., 2010; Turgeon and Brumsack, 2006; Turgeon and Creaser, 2008; Wang et al., 2001; Wilson and Norris, 2001; Zou et al., 2005). Currently available data suggest that the major forcing conditions behind OAEs were abrupt increases in global temperature (Suan et al., 2010; Wilson and Norris, 2001), induced by rapid ingrowth of CO_2 and/or methane into the atmosphere (Hesselbo et al., 2000; Jenkyns, 2010). Methane is a more effective greenhouse gas than CO_2 (Yang et al., 2013; Yu et al., 2007) and is eventually oxidized to CO_2 in the atmosphere. Both global warming and high atmospheric CO_2 are favorable for chemical weathering (Jenkyns, 2010). Meanwhile, elevated temperatures and CO_2 in the Phanerozoic may have led to blooming of plants and consequently rapid evolution of the whole biosphere. This in turn resulted in high oxygen levels in the atmosphere due to photosynthesis, followed by low temperatures as the greenhouse conditions eased, and then most importantly, the extreme conditions of the OAEs. The release of greenhouse gases, e.g., CO_2 from volcanic eruptions and/or methane from buried biomass, starts another warm-cool-OAE cycle. Therefore, high CO_2 warm and high O_2 cool periods usually appeared successively before OAEs (Suan et al., 2010). For example, a pronounced (~5 °C) cooling event was discovered in the Late Pliensbachian, which is followed by a remarkable ~7–10 °C seawater warming, then a second cooling event, and finally the OAE in the early Toarcian (Suan et al., 2010).

Highly fluctuating climate and hydrological cycles could dramatically enhance the chemical weathering, which,

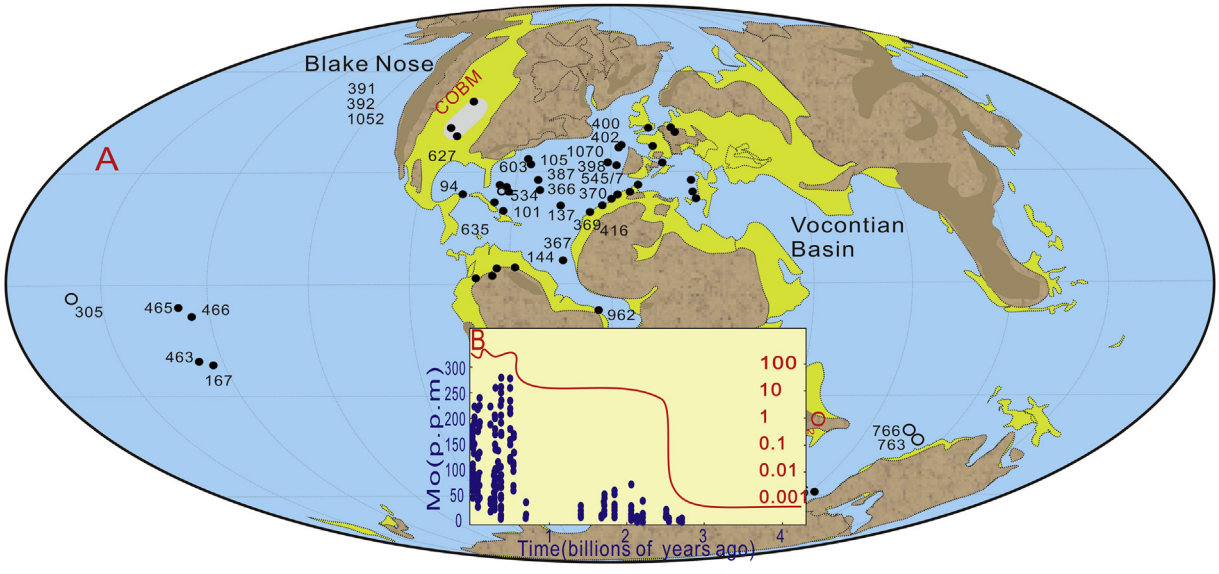

Fig. 2. Black shales and other organic rich sediments formed during OAEs in the Jurassic and the Cretaceous are widely distributed on the ocean floors of the Pacific (Robinson et al., 2004; Takashima et al., 2010), the Atlantic (Berrocoso et al., 2008; Lipinski et al., 2003) and the Tethys (McArthur et al., 2008). A. A sketch map of a plate reconstruction at the mid-Cretaceous period, showing the global location of sites with well-dated sections correlative to the upper Albian OAE (solid circles). Also shown are sites that show no obvious lithological expression of OAE (open circles) and the location of the Colorado Mineral Belt (COMB). Numbers refer to Deep Sea Drilling Project and Ocean Drilling Program Sites (modified after (Wilson and Norris, 2001)). The COMB was underwater behind the uplifting continental arc, which is favorable for Mo enriched sediments. B. A diagram of Mo contents (parts per million) in black shales versus age (billion year). Molybdenum is enriched in black shales younger than 550 Ma, corresponding to the abrupt increase in atmospheric oxygen (modified after (Kump, 2008; Scott et al., 2008)).

consequently, leads to release of Mo. During high oxygen periods before the OAEs, the released Mo was intensively oxidized to form water soluble MoO_4^{2-}, which would result in enhanced MoO_4^{2-} discharge to oceans and lakes. Given that Mo cannot be retained by sediments in oxic or even suboxic bottom waters (Turgeon and Brumsack, 2006), the Mo concentration in sea waters rose to much higher levels during warm high-oxygen periods than would occur under more temperate conditions. Subsequently, Mo was precipitated by interaction with organic-rich sediment during reducing conditions associated with the OAEs. Black shales and other organic-rich sediments formed during OAEs in the Jurassic and the Cretaceous are widely distributed in the Pacific (Robinson et al., 2004; Takashima et al., 2010), the Atlantic (Berrocoso et al., 2008; Lipinski et al., 2003) and the Tethys Ocean (McArthur et al., 2008; Wang et al., 2001). Molybdenum concentrations in anoxic sediments are up to several hundred times higher than those in the continental crust (Rimmer, 2004; Scott et al., 2008; Sun et al., 2015b) (Fig. 2).

In the East Pacific Ocean, conditions were perfect for concentration of Mo. Oceanic crust that formed during the period from Jurassic to Cretaceous, and even Cenozoic, was subducted, carrying with it Mo-rich sediments formed during the OAEs (Fig. 3). Some of the sediments may have been scraped off the slab, and accumulated in the accretion wedge during subduction. Some of the accreted sediments could have been subsequently entrained to deeper depths and metamorphosed through subduction entrainment, especially along erosive subduction margins (Vannucchi et al., 2008, 2013) (Fig. 4A). During plate subduction, organic materials release early. Therefore, metamorphosed organic-rich sediments have dramatically elevated oxygen fugacity (Sun et al., 2015b). Partial melting of these subducted and metamorphosed Mo-rich sediments is the most favorable process for the Cenozoic Mo porphyry deposits in the American continents. Hydrothermal activity and partial melting of the metamorphosed Mo-rich sediments lead to concentration of chalcophile elements in the fluids and deposition of highly enriched Mo ores.

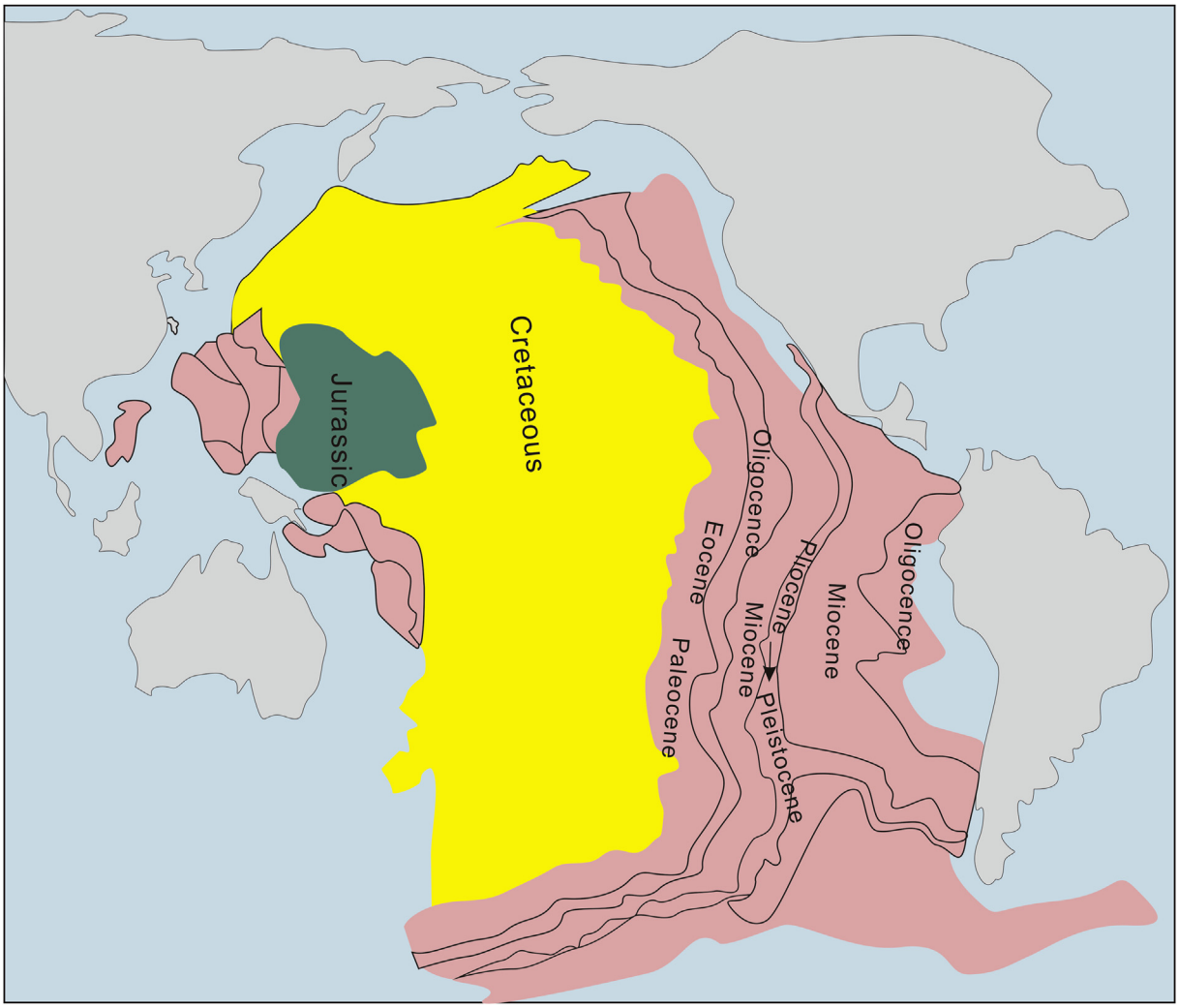

Fig. 3. The current age distribution of oceanic crust in the Pacific Ocean, showing that most of the Jurassic and Cretaceous oceanic crust in the east Pacific has been subducted, whereas little has been subducted in the west Pacific. Therefore, considerably more Mo-enriched sediments have been subducted along the east Pacific, through complicated processes of accretion and subduction erosion, carrying Mo into the mantle wedge.

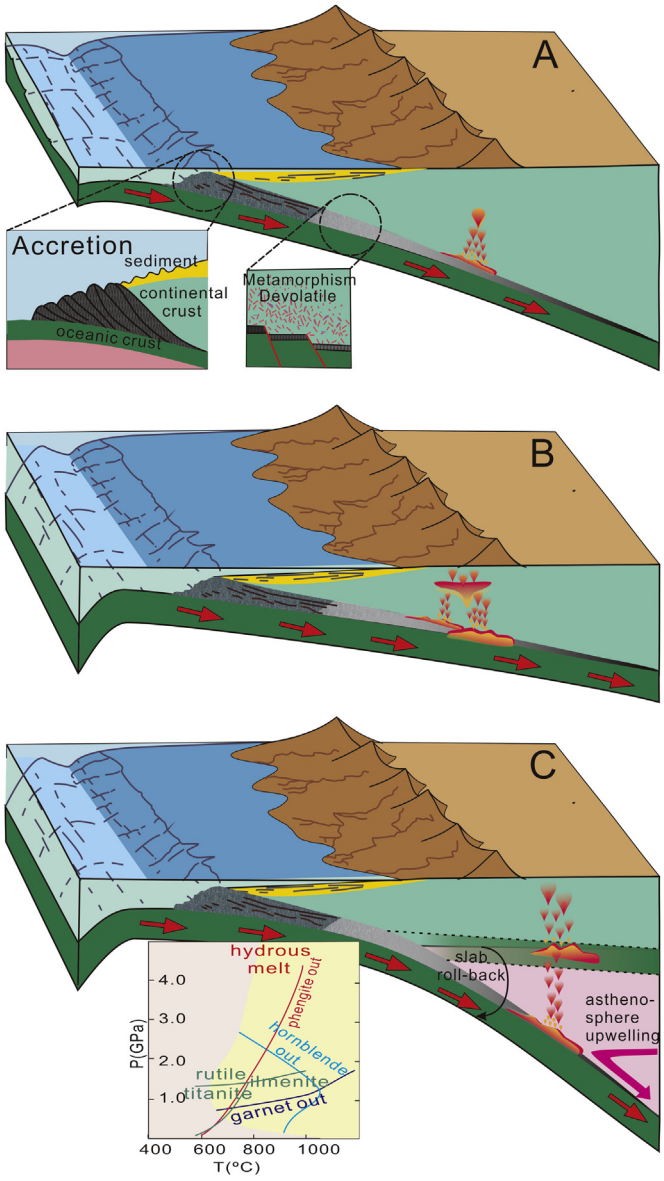

Fig. 4. Cartoons showing different subduction regimes and the formation of corresponding porphyry Mo deposits. A. Normal subduction and the formation of low-F porphyry Mo deposits. Most of the Mo-enriched sediments were scraped off the subducting slab, accreted in the fore-arc, and then entrained into the subduction zone through subduction erosion, followed by metamorphism. Partial melting of metamorphosed Mo-enriched sediments forms low-F porphyry Mo deposits. B. Subduction of young ridges generally takes more accreted and/or metamorphosed Mo-enriched sediments into the subduction zone through subduction erosion because of its rough surface and topography. Partial melting of subducting slab and sediments forms porphyry Cu–Mo deposits. C. Slab rollback causes elevated temperatures and induces the decomposition of phengite, and the transformation of titanite to ilmenite, thereby releasing F and Nb, Ta. Partial melting of the residue of Mo-enriched sediments (after early metamorphism and melt extraction) under such conditions forms high-F porphyry Mo deposits.

4. Different types of molybdenum deposits

There are three major types of Mo deposits along the west coast of the American continents – porphyry-Cu-Mo, high-F porphyry-Mo deposits, and low-F porphyry-Mo deposits. These deposits differ dramatically from each other in many aspects. Of the three types, porphyry-Cu-Mo deposits have the lowest Mo grades and the highest Cu, and Re concentrations. High-F (F commonly >1%) porphyry-Mo deposits have the highest Mo grades, with Re concentrations down to as low as ppm or tens of ppm in molybdenite, and essentially no Cu (Klemm et al., 2008; Stein et al., 2001). Low-F porphyry-Mo deposits have Mo grades slightly lower than high-F porphyry-Mo deposits, but with much lower F contents. Spatially and petrologically, low-F porphyry-Mo deposits are more likely porphyry-Cu deposits, but with Cu concentrations of less than 100 ppm.

4.1. Porphyry Cu–Mo deposits

These kind of deposits have very low Mo grades, ranging from 0.01 to 0.03 wt%, but may have large Mo reserves, e.g., El Teniente, 2.5 Mt, Chuquicamata, 1.81 Mt Mo metal (Cooke et al., 2005), ranking them in the top 5 Mo deposits in the world. Most of these porphyry-Cu-Mo deposits are diorite to granodiorite in composition and are closely associated with adakitic rocks (Sun et al., 2011), e.g., related to subduction of ridges or sea mount chains (aseismic ridge) (Ling et al., 2013, 2009; Sun et al., 2012a; Sun et al., 2010), which usually consist of young oceanic crust. These environments are the most favorable tectonic settings for slab melting (Defant and Drummond, 1990; Sun et al., 2011) under the cold geotherm present since the Phanerozoic. For example, the largest porphyry-Cu-Mo deposit, El Teniente, is spatially associated with the Juan Fernandez Ridge, whereas the second largest porphyry-Cu-Mo deposit, Chuquicamata, is associated with Iquique Ridge (Cooke et al., 2005) (Fig. 1); both were subducting at low angle underneath the South American continent (Sun et al., 2010).

From a geochemical point of view, the Mo/Cu of these deposits are fairly high (up to 0.04), which is more than 20 times higher than the primitive mantle value (1.7×10^{-3}) (McDonough and Sun, 1995) and ~7 times higher than the average MORB value (5.6×10^{-3}) (Arevalo and McDonough, 2010). Molybdenum abundance in MORB is only 0.39 ppm, whereas the estimated Cu abundance is 74 ppm (Arevalo and McDonough, 2010) or higher (~100 ppm) (Sun et al., 2003a). Given that Mo is only slightly more incompatible than Cu (Sun et al., 2003a, 2003b), pure slab melting can result in neither the Mo/Cu ratios nor the Mo contents of porphyry-Cu-Mo deposits if the host rocks are mostly andesitic in composition. The most favorable mechanism that forms porphyry-Cu-Mo deposits is partial melting of subducted oceanic crust with entrainment of Mo-rich sedimentary material (Fig. 5).

Molybdenum enriched sediments are much better entrained into the mantle in places where defects in the subducting plate occur, resulting in enhanced subduction erosion. Ridge subduction is one of the best places for sediment entrainment and subsequent partial melting during subduction because of its rough surface (Fig. 4B). It is also the best place for porphyry Cu mineralization because of slab melting (Sun et al., 2015b, 2013b). This plausibly explains the close association between Cu and Mo for porphyry-Cu-Mo deposits. The Mo/Cu ratio is

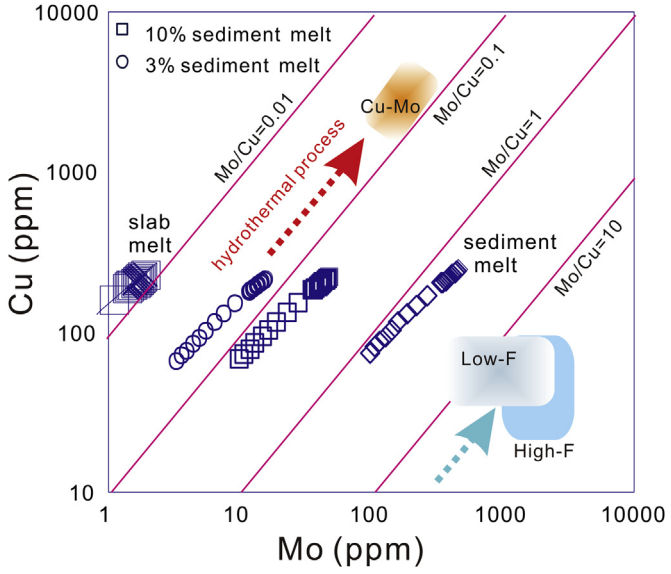

Fig. 5. A copper versus molybdenum diagram showing the distinctive differences among the three types of Mo deposits. Slab-melting forms magmas with very low Mo concentrations and Mo/Cu ratios lower than 0.01, which cannot explain the concentrations and Mo/Cu ratios of porphyry-Cu-Mo. The addition of several percent of sediment to slab melts can plausibly explain the Mo/Cu ratios of porphyry-Cu-Mo. Subsequent hydrothermal processes scavenge most of the Mo and Cu from magmas into sulfides, forming porphyry-Cu-Mo deposits. Low-F and high-F porphyry cannot be explained by direct partial melting of Mo enriched sediments. High-grade metamorphism is required to fractionate Mo from Cu, because Mo is presented as thiomolybdates whereas Cu as sulfide. Mid-ocean ridge basalt: Mo, 0.39 ppm, Cu, 70 ppm (Arevalo and McDonough, 2010); Mo rich sediment: Mo, 100 ppm, Cu, 75 ppm.

mainly controlled by the relative contributions of sediment melts versus slab melts, and Mo can be substantially diluted by slab melts, resulting in low Mo grades. Re is also a moderately incompatible element, marginally less incompatible than Mo (Sun et al., 2003a). The Re/Mo of the melts is established before high-grade metamorphism, and is close to that of the parental black shales. Therefore, molybdenite in this kind of deposit has high Re concentrations with Re/Mo comparable to that of subducted black shales (8×10^{-4} to 1.5×10^{-2}), equivalent to hundreds of ppm, and up to weight percent levels in molydenite assuming all the Mo and Re in magmas are scavenged into molybdenite. The high oxygen fugacity of these deposits can be interpreted by slab melting at convergent margins (Mungall, 2002), which promotes the release of chalcophile elements, e.g., Cu, Mo and Re from the subducting slab (Sun et al., 2003a, 2004). Most of the F in the subducting slab is retained in phengite and apatite at the early stage of plate subduction, and so porphyry-Cu-Mo deposits usually have low F contents.

4.2. High-F porphyry Mo deposits

This kind of porphyry Mo deposit is closely associated with shallowly intruded A-type high-silica rhyolites and granites. The total Mo reserves are comparable to those of giant porphyry-Cu-Mo deposits, but at much higher Mo grades (0.1–0.3% of Mo metal) (Klemm et al., 2008). The most famous high-F porphyry-Mo deposit belt in the world is Climax, which is located in the Colorado mineral belt. These deposits are associated with the volcanic and tectonic activities of the Tertiary Rio Grande rifting at the southeastern end of the Rocky Mountain chain, formed after peak activity of a magmatic cycle (Fig. 1).

Interestingly, these deposits are highly enriched in F (generally > 1%), rubidium (Rb, commonly > 500 ppm), and niobium (Nb)-tantalum (Ta) (Nb commonly > 50 ppm, with subchondritic Nb/Ta of ~10), but have strikingly low zirconium (Zr), strontium (Sr) and virtually no Cu or gold (Au) (Klemm et al., 2008). These characteristics have been used to argue that the ore-forming rocks were not produced during subduction, but by interaction of mantle-derived melts with high-grade metamorphic rocks at the base of the continental crust (Ludington and Plumlee, 2009). The problem is that pure mantle-derived melts generally have Mo concentrations in lower or sub-ppm levels. Moreover, it cannot plausibly explain the sub-chondritic Nb/Ta and the remarkably low Sr and Zr concentrations, either.

The high-F porphyries can be interpreted as forming by partial melting of high-grade metamorphosed Mo-rich sediments (with or without previous melt extraction) induced by heating during slab rollback (Fig. 4C). Metamorphosed sediments are also rich in phengite and other high-K minerals. Phengite in the subducting slab decomposes during the slab rollback because of the abruptly elevated geotherm (Li et al., 2012; Schmidt, 1996) and releases abundant F- and K-rich fluids, which may explain the high F and high K characteristics of porphyry Mo deposits. The high F contents dramatically lower the solidus of the magmas, producing compositions that are usually much more evolved than porphyry-Cu-Mo deposits (For example, the SiO_2 content of Jinduicheng porphyry Mo deposit goes up to ~75%). The slightly lower oxygen fugacity, relative to porphyry-Cu-Mo deposits (Fig. 1), is due to the absence of slab melts and normal arc magmas, which are more oxidizing in general (Sun et al., 2015a, 2015b, 2007b). Given that there are no Mo-poor slab melt components involved, as is the case for porphyry-Cu-Mo deposits, this kind of deposit usually has high Mo grades.

Black shales usually have Cu concentrations slightly higher than Mo, therefore, direct partial melting of Mo-rich black shales cannot form porphyry-Mo deposits without retaining Cu (Fig. 5). However, Mo is present as thiomolybdates in reducing sediments, whereas Cu appears mainly as sulfides (Tribovillard et al., 2006), hence major fractionation between Cu and Mo are expected during metamorphic and partial melting processes.

Shales are characterized by depletions of Nb, Ta, Sr and Zr, with Nb/Ta of about 12 (Barth et al., 2000). The partial melting of black shales may explain the striking depletion of Sr and Zr, but cannot explain the high Nb and Ta concentrations and the sub-chondritic Nb/Ta values of ~10. Niobium and Ta were previously taken as the most conservative elements during plate subduction (Pearce and Peate, 1995). However, Nb and Ta are highly mobile during the early stage

of plate subduction, before the appearance of rutile (Ding et al., 2013, 2009; Liang et al., 2009; Xiao et al., 2006). Fluids released during the blueschist to amphibolite transition have high Nb and Ta concentrations coupled with Nb/Ta as low as 5 (Ding et al., 2013, 2009; Xiao et al., 2006). Niobium and Ta are mostly hosted in titanite in metasomatised lithosphere at depths lower than 50 km, or rutile at deeper depths, and as such they are retained in the residue during partial melting of sediments at the early stage of plate subduction. Titanite transforms to ilmenite at high temperature (Liou et al., 1998). Rutile may also transform to ilmenite at high temperatures. Ilmenite has a much lower capacity for accepting Nb and Ta than titanite and rutile. Therefore, the rollback of the low-angle subducting plates leads to a titanite/rutile to ilmenite transition induced by elevated temperatures, resulting in release of Nb and Ta likely to F-rich fluids released during slab rollback. This then provides a feasible explanation of the high Nb, Ta characteristics of high-F porphyry-Mo deposits.

Previous studies have shown that the formation of the high-F porphyry Mo deposits in the Colorado mineral belt were closely associated with the volcanic and tectonic activities during the Tertiary Rio Grande rifting at the south end of the Rocky Mountain chain (Klemm et al., 2008; Ludington et al., 2009; Ludington and Plumlee, 2009). This in turn involved rollback of shallowly subducting oceanic lithosphere (Elston, 1984) along with mantle contributions (Farmer et al., 2008). Moreover, Pb isotopes reveal a high-grade metamorphic lower-crustal origin of the ore-forming magmas (Stein and Hannah, 1985), due to extension subsequent to cessation of subduction of the Kula and Farallon plates beneath western North America (Ludington and Plumlee, 2009). All these observations are compatible with our model.

Molybdenite in high-F porphyry-Mo deposits has Re concentrations in the lower teens to single digit part-per-million levels. This has been attributed to sourcing from the continental crust (Stein et al., 2001). The Re/Mo ratio of the continental crust (2.5×10^{-3} to 2.5×10^{-4}) (Rudnick and Gao, 2003; Sun et al., 2003b), however, corresponds to hundreds to thousands of ppm Re in molybdenite, because there is no major fractionation between these two moderately incompatible elements during magmatic processes.

Rhenium has a high accumulation potential even at slightly reducing conditions (Colodner et al., 1993), whereas Mo is not significantly enriched in sediments under even suboxic bottom waters (Turgeon and Brumsack, 2006). Therefore, Re/Mo is sensitive to redox conditions (Turgeon and Brumsack, 2006). Molybdenum-enriched sediments formed in reducing environments usually have lower Re/Mo ratios (Turgeon and Brumsack, 2006). In closed or semiclosed water bodies, Re/Mo decreases with increasing organic carbon contents (i.e. more reducing conditions). More fractionation between Re/Mo can be expected in places with higher redox gradients. Therefore, melting of metamorphosed sediments with higher organic contents results in low Re contents in molybdenite. Moreover, Mo-rich sediments lose more Re than Mo during metamorphism, because Re is highly volatile, much more volatile than Mo (Sun et al., 2003b), and can be released during devolatilization of the sediments (Becker, 2000). Therefore, molybdenite from high-F porphyry-Mo deposits has low Re concentrations. These characteristics explain the low Re concentrations in molybdenite from high-F porphyry-Mo deposits.

4.3. Low-F porphyry-Mo deposits

These kinds of Mo deposits are widely distributed in the North American Cordillera (Fig. 1), and are attributed to the subduction of the Kula and Farallon plates beneath western North America. In contrast to porphyry-Cu-Mo and high-F porphyry-Mo deposits, which formed mainly in the Cenozoic, low-F porphyry-Mo deposits on the west coast of North America formed over a wider time interval from 144 to 8 Ma, with about half of the reserves forming in the Cenozoic (Ludington et al., 2009). This kind of deposit is usually large, with grades of 0.05–0.2 percent Mo, which is lower than those of high-F porphyry-Mo deposits, but considerably higher than those of porphyry-Cu-Mo deposits (Fig. 5). Generally, low-F porphyry-Mo deposits do not form in the same regions or tectonic environments as Climax-type high-F porphyry-Mo deposits, but are rather closely related to porphyry-Cu deposits. For example, both low-F porphyry-Mo and porphyry-Mo-Cu deposits are associated with igneous rocks in continental-margin subduction-related magmatic arcs along the west coast of the American continents, i.e., they formed in the same regions and at the same times (Ludington et al., 2009). The high Mo grades indicate involvement of Mo-rich black shales, whereas the low Cu contents (generally < 100 ppm), compared to porphyry-Cu-Mo deposits, indicate limited contributions from slab melts. Low-F porphyry-Mo deposits are less felsic, with lower F, Nb, and Ta concentrations, and slightly lower Mo grades than high-F porphyry-Mo deposits. The most straightforward explanation of their origin is through partial melting of metamorphosed Mo-rich sediments that have been entrained into the mantle wedge through subduction erosion. Both black shales and arc magmas are depleted in Nb and Ta, such that low-F porphyry-Mo deposits have low Nb and Ta concentrations, while lower F leads to a higher solidus temperature, more mafic magmas, and consequently lower Mo grades compared to high-F porphyry-Mo deposits. This also explains the spatial association between porphyry-Cu and low-F porphyry-Mo deposits. The key factor that controls low-F porphyry-Mo is not flat subduction, but the availability of Mo-rich sediments. About half of the low-F porphyry-Mo reserves in the west American continental margin formed in the Cretaceous, which is distinctively older than high-F porphyry-Mo and porphyry-Cu-Mo deposits.

5. Discussion

In contrast to the eastern Pacific margin, the western Pacific island arcs contain far fewer Mo deposits (Fig. 1). There is essentially no porphyry in the northwest Pacific arc, whereas porphyry deposits in southwest Pacific island arcs are mostly

porphyry Cu–Au deposits (Sillitoe, 2010; Sun et al., 2012a; Zhan et al., 2015). Sepon is the only deposit that has Mo (Fig. 1). It is however, mainly a skarn-type deposit with porphyry mineralizations (Sillitoe, 2010), located in a backarc setting. The dramatic differences between the east and west Pacific margins are due to different subduction regimes in the east and west Pacific.

First of all, backarc basins were better developed along the western Pacific margins. These are more reducing than open oceans, and thus would have lower Mo, Re as well as nutrients (Fig. 6). This is supported by the limited development of sequences of black shales in the western Pacific during the early Aptian OAE (Jenkyns, 2010). For example, some OAE events are not recorded on Shatsky Rise in the northwest Pacific. “Black shale" deposition in the Pacific Ocean was only possible when a “carbon-burial threshold" was crossed (Robinson et al., 2004).

In addition, the drifting history of the Pacific and Farallon plates are quite different (Koppers et al., 2001, 2003; Seton et al., 2012; Sun et al., 2007a, 2013a; Torsvik et al., 2010), which resulted in the development of an asymmetric Pacific Ocean floor (Fig. 3). The Pacific plate was drifting northward from ~100 to 50 Ma (Beaman et al., 2007; Sun et al., 2007a), such that there was not much westward subduction during this period. Therefore, little Mo-rich sediment has been subducted to the mantle wedge underneath the west Pacific island arcs. In contrast, the Farallon plate was drifting eastward at least since the Cretaceous (Ernst, 2010; Ernst et al., 2008; Torsvik et al., 2010). As a result, most of the oceanic crust that formed before the Late Cretaceous has abundant surficial Mo-rich sediments and these have been subducted in the eastern Pacific, adding Mo to the mantle wedge.

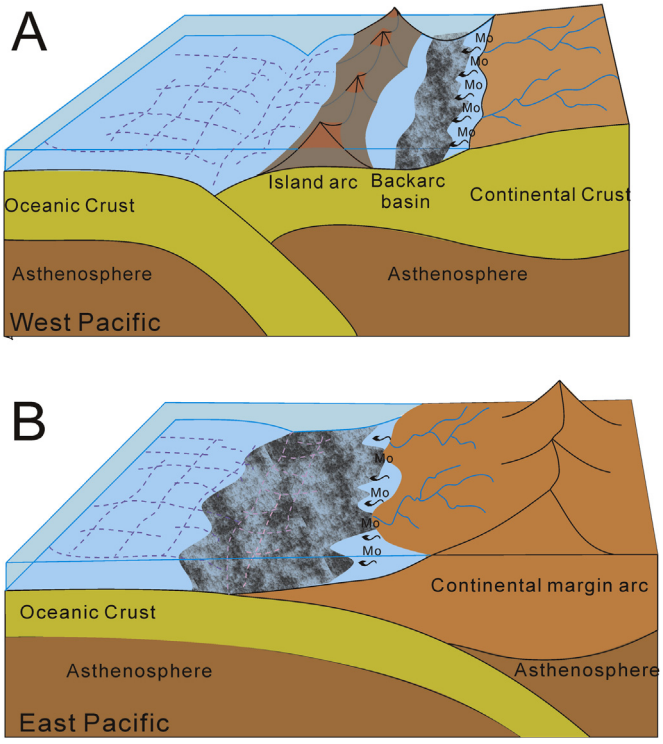

Fig. 6. Cartoons showing the difference between the east and west Pacific margins. In the East, subduction is flat to low angle with a continental-margin arc versus steep subduction with a backarc basin in the west. A. Backarc basins in the west Pacific hindered the transportation of Mo, Re as well as nutrients to the Pacific Ocean, forming less Mo enriched sediments there. B. Fluvial input and redox states are the controlling factors for Mo-enriched sediments, therefore off-shore environments are more favorable than open oceans for Mo enrichment.

Moreover, young, hot oceanic crust is subducting though low angle or flat subductions in the east Pacific, such that there is considerably more partial melting of the subducting slab (Defant and Drummond, 1990) and porphyry mineralization (Sun et al., 2012a, 2012b, 2011) and presumably also partial melting of metasediments. Flat/low angle subduction results in stronger subduction erosion, which takes in more metamorphosed Mo-rich sediments, forming more porphyry Cu–Mo, and pure porphyry Mo deposits. In contrast, the west Pacific is dominated by Cretaceous oceanic crust with some Jurassic oceanic crust to the east of the Phillipine Sea (Fig. 3). The subduction angles are usually much steeper than those in the east Pacific margin. There is essentially no slab melting and so less Mo has been injected into the mantle wedge in the west Pacific, such that there are no porphyry Cu–Mo nor porphyry Mo deposits. Porphyry-Cu (Au) deposits in the west Pacific are all associated with young backarc basins with ridge subductions (Cooke et al., 2005; Sun et al., 2010; Zhan et al., 2015). Given that these young backarc basin crusts are all younger than 55 Ma, i.e. the last OAE (55.8 Ma) (Jenkyns, 2010), these porphyry Cu deposits have no Mo (Fig. 1) (Sillitoe, 2010).

6. Conclusions

(1) The oxidation–reduction-cycle and subduction style are the key factors for Mo porphyry mineralization. Molybdenum is more intensively oxidized under high erosion rates during alternating high atmospheric-CO_2 and oxygen-rich periods immediately before Oceanic Anoxic Events, resulting in high Mo concentrations in surface water and consequently higher Mo concentrations in organic rich sediments.

(2) The uneven distribution of Mo deposits in the circum-Pacific region is mainly due to the different subduction regimes in the east and west Pacific margins. Far more Mo-rich sediments formed and subsequently subducted in the east Pacific.

(3) Molybdenum deposits in the east Pacific margin can be classified into three types, porphyry-Cu-Mo, high- F porphyry-Mo, and low-F porphyry-Mo deposits. Porphyry-Cu-Mo deposits are usually associated with ridge subductions, and thus formed through partial melting of subducted oceanic crust and metamorphosed Mo-rich sedimentary material due to subduction erosion. The high-F porphyry-Mo deposits are formed by partial melting of high-grade metamorphosed Mo-rich sediments on the subducting slab during slab rollback. Low-F porphyry-Mo deposits are formed through direct partial

melting of metamorphosed Mo-rich sediments entrained into the mantle wedge through subduction erosion.

Acknowledgment

The contribution is supported by Ministry of Science and Technology of China (2012CB416703), the Natural Science Foundation of China (No. 41090374, 41421062). Constructive review comments from Dr. E.S. Cheney and F.Z. Teng are highly appreciated. Contribution No. IS-xxxx from GIGCAS.

References

Alberdi-Genolet, M., Tocco, R., 1999. Trace metals and organic geochemistry of the machiques member (Aptian-Albian) and La luna formation (Cenomanian-Campanian), Venezuela. Chem. Geol. 160 (1−2), 19−38.

Arevalo, R., McDonough, W.F., 2010. Chemical variations and regional diversity observed in MORB. Chem. Geol. 271 (1−2), 70−85.

Barth, M.G., McDonough, W.F., Rudnick, R.L., 2000. Tracking the budget of Nb and Ta in the continental crust. Chem. Geol. 165 (3−4), 197−213.

Beaman, M., Sager, W.W., Acton, G.D., Lanci, L., Pares, J., 2007. Improved late cretaceous and early cenozoic paleomagnetic apparent polar wander path for the Pacific plate. Earth Planet. Sci. Lett. 262 (1−2), 1−20.

Becker, H., 2000. Re-Os fractionation in eclogites and blueschists and the implications for recycling of oceanic crust into the mantle. Earth Planet. Sci. Lett. 177 (3−4), 287−300.

Berrocoso, A.J., MacLeod, K.G., Calvert, S.E., Elorza, J., 2008. Bottom water anoxia, inoceramid colonization, and benthopelagic coupling during black shale deposition on Demerara rise (Late cretaceous western tropical North Atlantic). Paleoceanography 23 (3).

Chen, Y.J., Li, C., Zhang, J., Li, Z., Wang, H.H., 2000. Sr and O isotopic characteristics of porphyries in the qinling molybdenum deposit belt and their implication to genetic mechanism and type. Sci. China Ser. D Earth Sci. 43, 82−94.

Colodner, D., et al., 1993. The geochemical cycle of rhenium − a reconnaissance. Earth Planet. Sci. Lett. 117 (1−2), 205−221.

Cooke, D.R., Hollings, P., Walsh, J.L., 2005. Giant porphyry deposits: characteristics, distribution, and tectonic controls. Econ. Geol. 100 (5), 801−818.

Defant, M.J., Drummond, M.S., 1990. Derivation of some modern arc magmas by melting of young subducted lithosphere. Nature 347, 662−665.

Ding, X., et al., 2013. Major Nb/Ta fractionation recorded in garnet amphibolite facies metagabbro. J. of Geol. 121 (3), 255−274.

Ding, X., et al., 2009. Natural and experimental constraints on formation of the continental crust based on niobium−tantalum fractionation. Int. Geol. Rev. 51 (6), 473−501.

Elston, W.E., 1984. Subduction of young oceanic lithosphere and extensional orogeny in southwestern North America during mid-tertiary time. Tectonics 3, 229−250.

Ernst, W.G., 2010. Late mesozoic subduction-induced hydrothermal gold deposits along the eastern Asian and northern Californian margins: oceanic versus continental lithospheric underflow. Isl. Arc 19 (2), 213−229.

Ernst, W.G., Snow, C.A., Scherer, H.H., 2008. Contrasting early and late mesozoic petrotectonic evolution of northern California. Geol. Soc. Am. Bull. 120 (1−2), 179−194.

Farmer, G.L., Bailley, T., Elkins-Tanton, L.T., 2008. Mantle source volumes and the origin of the mid-tertiary ignimbrite flare-up in the southern rocky mountains, western US. Lithos 102 (1−2), 279−294.

Hesselbo, S.P., et al., 2000. Massive dissociation of gas hydrate during a Jurassic oceanic anoxic event. Nature 406 (6794), 392−395.

Jenkyns, H.C., 2010. Geochemistry of oceanic anoxic events. Geochem. Geophys. Geosystems 11.

Jiang, S.Y., et al., 2009. Early Cambrian ocean anoxia in South China. Nature 459 (7248), E5−E6.

Klemm, L.M., Pettke, T., Heinrich, C.A., 2008. Fluid and source magma evolution of the Questa porphyry Mo deposit, New Mexico, USA. Miner. Deposita 43 (5), 533−552.

Koppers, A.A.P., Morgan, J.P., Morgan, J.W., Staudigel, H., 2001. Testing the fixed hotspot hypothesis using $^{40}Ar/^{39}Ar$ age progressions along seamount trails. Earth Planet. Sci. Lett. 185 (3−4), 237−252.

Koppers, A.A.P., Staudigel, H., Duncan, R.A., 2003. High-resolution $^{40}Ar/^{39}Ar$ dating of the oldest oceanic basement basalts in the western Pacific basin. Geochem. Geophys. Geosystems 4. ISI:000186939000001.

Kump, L.R., 2008. The rise of atmospheric oxygen. Nature 451 (7176), 277−278.

Li, C.Y., et al., 2012. Formation of the world's largest molybdenum metallogenic belt: a plate-tectonic perspective on the Qinling molybdenum deposits. Int. Geol. Rev. 54 (9), 1093−1112.

Li, N., et al., 2007. Molybdenum deposits in east qinling. Earth Sci. Front. 14 (05), 186−198 (in Chinese with English abstract).

Liang, J.L., et al., 2009. Nb/Ta fractionation observed in eclogites from the Chinese continental scientific drilling project. Chem. Geol. 268 (1−2), 27−40.

Ling, M.X., et al., 2013. Destruction of the North China craton induced by ridge subductions. J. Geol. 121 (2), 197−213.

Ling, M.X., et al., 2009. Cretaceous ridge subduction along the lower Yangtse river Belt, eastern China. Econ. Geol. 104 (2), 303−321.

Liou, J.G., Zhang, R.Y., Ernst, W.G., Liu, J., McLimans, R., 1998. Mineral parageneses in the Piampaludo eclogitic body, Gruppo di Voltri, Western Ligurian Alps. Schweiz. Mineral. Und Petrogr. Mittl. 78 (2), 317−335.

Lipinski, M., Warning, B., Brumsack, H.J., 2003. Trace metal signatures of Jurassic/Cretaceous black shales from the Norwegian shelf and the barents sea. Palaeogeogr. Palaeoclimatol. Palaeoecol. 190, 459−475.

Ludington, S., Hammarstrom, J., Piatak, N., 2009. Low-fluorine Stockwork Molybdenite Deposits. US Geological Survey, Reston.

Ludington, S., Plumlee, G.S., 2009. Climax-Type Porphyry Molybdenum Deposits. US Geological Survey, Reston.

Ma, J.L., Wei, G.H., Xu, Y.G., Long, W.G., Sun, W.D., 2007. Mobilization and re-distribution of major and trace elements during extreme weathering of basalt in Hainan Island, South China. Geochimica Cosmochimica Acta 71 (13), 3223−3237.

Mao, J.W., et al., 2002. Re-Os dating of polymetallic Ni−Mo−PGE−Au mineralization in lower Cambrian black shales of south China and its geologic significance. Econ. Geol. Bull. Soc. Econ. Geol. 97 (5), 1051−1061.

McArthur, J.M., Algeo, T.J., van de Schootbrugge, B., Li, Q., Howarth, R.J., 2008. Basinal restriction, black shales, Re−Os dating, and the early Toarcian (Jurassic) oceanic anoxic event. Paleoceanography 23 (4).

McDonough, W.F., Sun, S.S., 1995. The composition of the earth. Chem. Geol. 120 (3−4), 223−253.

McElwain, J.C., Wade-Murphy, J., Hesselbo, S.P., 2005. Changes in carbon dioxide during an oceanic anoxic event linked to intrusion into Gondwana coals. Nature 435 (7041), 479−482.

Mungall, J.E., 2002. Roasting the mantle: slab melting and the genesis of major Au and Au-rich Cu deposits. Geology 30 (10), 915−918.

Pearce, J.A., Peate, D.W., 1995. Tectonic implications of the composition of volvanic arc magmas. Annu. Rev. Earth Planet. Sci. 23, 251−285.

Rimmer, S.M., 2004. Geochemical paleoredox indicators in Devonian-Mississippian black shales, central Appalachian basin (USA). Chem. Geol. 206 (3−4), 373−391.

Robinson, S.A., Williams, T., Bown, P.R., 2004. Fluctuations in biosiliceous production and the generation of early cretaceous oceanic anoxic events in the Pacific Ocean (Shatsky Rise, Ocean drilling program leg 198). Paleoceanography 19 (4).

Rudnick, R.L., Gao, S., 2003. Composition of the continental crust. In: Heinrich, D.H., Turekian, K.K. (Eds.), Treatise on Geochemistry. Pergamon, Oxford, pp. 1−64.

Schmidt, M.W., 1996. Experimental constraints on recycling of potassium from subducted oceanic crust. Science 272 (5270), 1927−1930.

Scopelliti, G., Bellanca, A., Neri, R., Baudin, F., Coccioni, R., 2006. Comparative high-resolution chemostratigraphy of the Bonarelli level from the reference Bottaccione section (Umbria-Marche Apennines) and from

an equivalent section in NW Sicily: consistent and contrasting responses to the OAE2. Chem. Geol. 228 (4), 266−285.
Scott, C., et al., 2008. Tracing the stepwise oxygenation of the proterozoic ocean. Nature 452 (7186), 456−459.
Seton, M., et al., 2012. Global continental and ocean basin reconstructions since 200 Ma. Earth Sci. Rev. 113 (3−4), 212−270.
Sillitoe, R.H., 2010. Porphyry copper systems. Econ. Geol. 105 (1), 3−41.
Stein, H.J., Hannah, J.L., 1985. Movement and origin of ore fluids in climax-type systems. Geology 13 (7), 469−474.
Stein, H.J., Markey, R.J., Morgan, J.W., Hannah, J.L., Schersten, A., 2001. The remarkable Re−Os chronometer in molybdenite: how and why it works. Terra Nova 13 (6), 479−486.
Suan, G., et al., 2010. Secular environmental precursors to early Toarcian (Jurassic) extreme climate changes. Earth Planet. Sci. Lett. 290 (3−4), 448−458.
Sun, S.S., McDonough, W.F., 1989. Chemical and isotopic systematics of oceanic basalts; implications for mantle composition and processes. In: Saunders, A.D., Norry, M.J. (Eds.), Magmatism in the Ocean Basins. Geological Society Special Publications. Geological Society of London, London, United Kingdom, pp. 313−345.
Sun, W.D., Bennett, V.C., Eggins, S.M., Arculus, R.J., Perfit, M.R., 2003a. Rhenium systematics in submarine MORB and back-arc basin glasses: laser ablation ICP-MS results. Chem. Geol. 196 (1−4), 259−281.
Sun, W.D., Bennett, V.C., Eggins, S.M., Kamenetsky, V.S., Arculus, R.J., 2003b. Enhanced mantle-to-crust rhenium transfer in undegassed arc magmas. Nature 422 (6929), 294−297.
Sun, W.D., Bennett, V.C., Kamenetsky, V.S., 2004. The mechanism of Re enrichment in arc magmas: evidence from Lau basin basaltic glasses and primitive melt inclusions. Earth Planet. Sci. Lett. 222 (1), 101−114.
Sun, W.D., Ding, X., Hu, Y.H., Li, X.H., 2007a. The golden transformation of the cretaceous plate subduction in the west Pacific. Earth Planet. Sci. Lett. 262 (3−4), 533−542.
Sun, W.D., et al., 2015a. Porphyry deposits and oxidized magmas. Ore Geol. Rev. 65, 97−131.
Sun, W.D., et al., 2015b. The geochemical behavior of molybdenum and mineralization. Acta Petrol. Sin. 31 (7).
Sun, W.D., et al., 2013a. Large-scale gold mineralization in eastern China induced by an early cretaceous clockwise change in Pacific plate motions. Int. Geol. Rev. 55 (3), 311−321.
Sun, W.D., et al., 2013b. The link between reduced porphyry copper deposits and oxidized magmas. Geochim. Cosmochim. Acta 103, 263−275.
Sun, W.D., et al., 2012a. Geochemical constraints on adakites of different origins and copper mineralization. J. Geol. 120 (1), 105−120.
Sun, W.D., et al., 2012b. The genetic association of adakites and Cu−Au ore deposits: a reply. Int. Geol. Rev. 54 (3), 370−372.
Sun, W.D., et al., 2010. Ridge subduction and porphyry copper−gold mineralization: an overview. Sci. China Earth Sci. 53 (4), 475−484.
Sun, W.D., et al., 2011. The genetic association of adakites and Cu−Au ore deposits. Int. Geol. Rev. 53 (5−6), 691−703.
Sun, X.M., et al., 2007b. Monazite, iron oxide and barite exsolutions in apatite aggregates from CCSD drillhole eclogites and their geological implications. Geochim. Cosmochim. Acta 71 (11), 2896−2905.
Takashima, R., et al., 2010. High-resolution terrestrial carbon isotope and planktic foraminiferal records of the upper cenomanian to the lower campanian in the Northwest Pacific. Earth Planet. Sci. Lett. 289 (3−4), 570−582.
Torsvik, T.H., Steinberger, B., Gurnis, M., Gaina, C., 2010. Plate tectonics and net lithosphere rotation over the past 150 My. Earth Planet. Sci. Lett. 291 (1−4), 106−112.
Tribovillard, N., Algeo, T.J., Lyons, T., Riboulleau, A., 2006. Trace metals as paleoredox and paleoproductivity proxies: an update. Chem. Geol. 232 (1−2), 12−32.
Turgeon, S., Brumsack, H.J., 2006. Anoxic vs dysoxic events reflected in sediment geochemistry during the Cenomanian-Turonian boundary event (Cretaceous) in the Umbria-Marche BASIN of central Italy. Chem. Geol. 234 (3−4), 321−339.
Turgeon, S.C., Creaser, R.A., 2008. Cretaceous oceanic anoxic event 2 triggered by a massive magmatic episode. Nature 454 (7202), 323−326.
Vannucchi, P., Remitti, F., Bettelli, G., 2008. Geological record of fluid flow and seismogenesis along an erosive subducting plate boundary. Nature 451 (7179), 699−703.
Vannucchi, P., et al., 2013. Rapid pulses of uplift, subsidence, and subduction erosion offshore Central America: implications for building the rock record of convergent margins. Geology 41 (9), 995−998.
Wang, C.S., Hu, X.M., Jansa, L., Wan, X.Q., Tao, R., 2001. The Cenomanian-Turonian anoxic event in southern Tibet. Cretac. Res. 22 (4), 481−490.
Wille, M., Nagler, T.F., Lehmann, B., Schroder, S., Kramers, J.D., 2008. Hydrogen sulphide release to surface waters at the Precambrian/Cambrian boundary. Nature 453 (7196), 767−769.
Wilson, P.A., Norris, R.D., 2001. Warm tropical ocean surface and global anoxia during the mid-Cretaceous period. Nature 412 (6845), 425−429.
Xiao, Y.L., et al., 2006. Making continental crust through slab melting: constraints from niobium-tantalum fractionation in UHP metamorphic rutile. Geochim. Cosmochim. Acta 70 (18), 4770−4782.
Yang, W.-B., et al., 2013. Isotopic evidence for continental ice sheet in mid-latitude region in the supergreenhouse early Cretaceous. Sci. Rep. 3 http://dx.doi.org/10.1038/srep02732.
Yu, J.B., et al., 2007. Enhanced net formations of nitrous oxide and methane underneath the frozen soil in Sanjiang wetland, northeastern China. J. Geophys. Res. Atmos. 112 (D7). ISI:000245727900002.
Zhan, M.Z., Sun, W.D., Ling, M.X., Li, H., 2015. Huangyan ridge subduction and formation of porphyry Cu−Au deposits in Luzon. Acta Petrol. Sin. 31 (7), 2101−2114.
Zhang, H., et al., 2014. Shapinggou: the largest climax-type porphyry Mo deposit in China. Int. Geol. Rev. 56 (3), 313−331.
Zou, Y.R., Kong, F., Peng, P.A., Hu, X.M., Wang, C.S., 2005. Organic geochemical characterization of upper cretaceous oxic oceanic sediments in Tibet, China: a preliminary study. Cretac. Res. 26 (1), 65−71.